J Mater Sci: Mater Med (2010) 21:2125–2132
DOI 10.1007/s10856-010-4075-8

Preparation of a novel biodegradable nanocomposite scaffold based on poly (3-hydroxybutyrate)/bioglass nanoparticles for bone tissue engineering

Hadi Hajiali · Saeed Karbasi · Mohammad Hosseinalipour · Hamid Reza Rezaie

Received: 25 October 2009 / Accepted: 29 March 2010 / Published online: 7 April 2010

Abstract One of the most important challenges in composite scaffolds is pore architecture. In this study, poly (3-hydroxybutyrate) with 10% bioglass nanoparticles was prepared by the salt leaching processing technique, as a nanocomposite scaffold. The scaffolds were characterized by SEM, FTIR and DTA. The SEM images demonstrated uniformed porosities of appropriate sizes (about 250–300 μm) which are interconnected. Furthermore, higher magnification SEM images showed that the scaffold possesses less agglomeration and has rough surfaces that may improve cell attachment. In addition, the FTIR and DTA results showed favorable interaction between polymer and bioglass nanoparticles which improved interfaces in the samples. Moreover, the porosity of the scaffold was assessed, and the results demonstrated that the scaffold has uniform and high porosity in its structure (about 84%). Finally it can be concluded that this scaffold has acceptable porosity and morphologic character paving the way for further studies to be conducted from the perspective of bone tissue engineering.

1 Introduction

There are over 500,000 bone repair procedures performed yearly, as a result of bone defects and non-unions caused by trauma, tumor, infection or abnormal progression [1]. Current surgical methods of treating bony deficits such as autografts, allografts or metallic implants, confront considerable restrictions [2, 3]. Although autografts have the characteristic benefit of biocompatibility without the dangers of disease transfer and are still the best approach for bone repair. However, their limited availability necessitates improvement in alternative bone replacement methods. One alternative is allogenic bone grafts that are more available than autografts and prevent the necessity for a second surgical procedure to obtain an autograft. However, the utilization of allogenic bone grafts may transmit diseases and induce immune responses, which can lead to graft rejection [4].

Over the past decade, tissue engineering has been widely inspected as a promising approach towards regeneration of bone tissue [5]. Biomaterials are necessary in tissue engineering strategies for the manufacture of scaffolds where pertinent cells attach, grow, proliferate and differentiate [6]. Thus, as the main target, bone tissue engineering has applied developed biodegradable materials as bone graft substitutes for filling large bone defects [7, 8]. In bone tissue engineering, scaffold serves as the matrices of tissue formation and plays a pivotal role. Thus the choice of the most appreciated material to produce a scaffold is an indispensably important step in the construction of a tissue-engineered product, since its characteristics will identify the properties of the scaffold [9–12].

Polyhydroxyalkanoates (PHAs) are a class of biodegradable polyesters that have been used in combination or alone for biomedical applications such as sutures, repair devices, repair patches, slings, cardiovascular patches, orthopedic pins, adhesion barriers, stents, guided tissue repair/regeneration devices, articular cartilage repair devices, nerve guides, tendon repair devices, bone marrow

H. Hajiali · M. Hosseinalipour · H. R. Rezaie
Biomaterial Group, School of Metallurgy and Materials Engineering, Iran University of Science and Technology (IUST), Narmak, Tehran, Iran

S. Karbasi (✉)
Medical Physics and Biomedical Engineering Group, School of Medicine, Isfahan University of Medical Science, Isfahan, Iran
e-mail: karbasi@med.mui.ac.ir

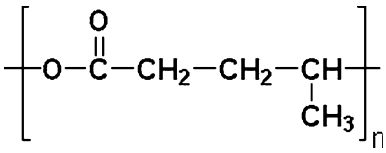

Fig. 1 The structure of PHB

scaffolds, and wound dressings [13–16]. Poly (3-hydroxybutyrate), as a member of the polyhydroxyalkanoates family, known as PHB, has attracted much attention for a variety of medical applications because of its biodegradation which exhibits a much longer degradation time than polymers of the poly (a-hydroxyacid) group (e.g. PLA or PLGA) and its excellent biocompatibility which has a good degree with various cell lines (Fig. 1) [16–24]. Furthermore, PHB has been reported to have piezoelectric properties which can possibly play a crucial role in stimulating bone growth and regeneration [25, 26]; it could also be used for bone tissue repair and as an effective agent against osteoporosis [27].

Several composites of PHB and bioactive inorganic phases, like hydroxyapatite, wollastonite and bioglass, have been produced to give strength and bioactivity to the composites [28, 29]. Inorganic phases can be augmented to the polymer matrix in their micro- or nanosize. However, for PHB composites, mainly microparticles have been investigated [28–32].

Recently, nanotechnology and its production have been utilized in a wide variety of medical engineering applications. Nanoscience is particularly useful in tissue engineering since the interactions between cells and biomaterials occur in nanoscale and the components of biological tissues are nanomaterials [33]. Nanoscales of hydroxyapatite [34–36], tricalcium phosphate [37–39], bioactive glass [40–44], titanium oxide [45–47], carbon nanotubes [48, 49] and diamonds [50], for example, have been prepared and used as reinforcement materials in biopolymer matrix composites. The greater specific surface area of the nanoparticles should lead to higher interface effects and also cause improved bioactivity and mechanical properties when compared to micro size particles [34, 37, 38, 40]. In addition, their utilization in a polymeric matrix closely mimics the structure of a natural bone [51].

In this study, a nano bioglass reinforced poly (3-hydroxybutyrate) composite scaffold was successfully prepared using the salt leaching process. The reason for using bioglass particles is their excellent osteoconductivity and high bioactivity [52–57], particularly in the form of nanoparticles [40, 41, 43, 58]. The nanocomposite scaffold was characterized by SEM, FTIR and DTA. The morphology of porosity in the scaffold was examined by SEM and the volume fraction of porosity was also assessed. The nanostructure was evaluated by high magnification SEM images.

2 Materials and methods

2.1 Materials

Poly (3hydroxybutyrate) was purchased from Sigma-Aldrich (USA, CAS NUMBER: 26063-00-3, LOT NUMBER: S68924-099), NaCl and chloroform from Merk (Germany). Also Tetraethylorthosilicate (TEOS, Merck) as silica precursor, Hydrogen ammonium phosphate (Merck) as phosphorus precursor, and Calcium nitrate (Merck) as calcium precursor were prepared. Nano bioglass was produced as described by Fathi et al. [58]. The TEOS and Ethanol were mixed and then distilled water was added to the solution under magnet stirrer and allowed to combine until the solution became clear. The H_2O: (TEOS) molar ratio was 12:1. After 30 min, hydrogen ammonium phosphate was added to the stirring solution, and after another 20 min, calcium nitrate was added and the solution was stirred for an additional hour. On completion of the hydrolysis procedure, the sols were aged in a drying oven at 50°C to reach a high viscosity near gelling point. The composition of the prepared bioactive glass is shown in Table 1.

2.2 Preparation of scaffold

PHB/bioglass nanocomposite scaffold was prepared using a combination of published salt-leaching techniques [14]. Briefly, 2 g PHB and 0.2 g nano bioglass were dissolved in chloroform with 6% w/v and refluxed at 60°C for 6 h. Then, they were sonicated for 30 min using a sonicating probe, and subsequently, the solution was poured into a bed of sieved sodium chloride particles 250–300 μm and the sodium chloride: polymer weight ratio was 90:10. The scaffold was placed under vacuum in a desiccator for 24 h for the solvent to evaporate completely. Then it was rinsed with distilled water for leaching the salt. After the salt-leaching process, the microporous polymer scaffold was obtained and then vacuum dried.

Table 1 The composition of nano bioglass

	CaO (%)	SiO_2 (%)	P_2O_5 (%)
Composition of nano bioglass	57.44	35.42	7.15

2.3 Scanning electron microscopy (SEM)

Some scaffolds were broken in liquid nitrogen to probe a cross section area. Then the samples were mounted on aluminum stumps, gold coated in a sputtering device, and then examined using a scanning electron microscope (XL30, Philips co. Holland) for pore structure study. SEM images were taken at various magnifications and acceleration voltages (max. of 15 kV) to avoid beam damage to the polymer.

2.4 ATR-FTIR analysis

To characterize the surface of modified samples, attenuated total reflectance Fourier transform infrared (ATR-FTIR) analysis was performed using a FT-IR instrument (BRUKER) with a ZnSe prism.

2.5 Differential thermal analysis (DTA)

To evaluate the interface bond of nanocomposite phases, differential thermal analysis (Shimadzu system) was carried out on air from room temperatures up to 500°C, with a heating rate of 10°C/min in a Pt crucible.

2.6 Determination of porosity

The weight (W_d) and volume (V_s) of dried scaffold was measured and then the scaffold was immersed in deionized water overnight. Then, the weight of wet scaffold (W_w) was measured. The weight of water absorption in the pores of the scaffolds was determined by subtracting the scaffold's dry weight (W_d) from W_w. The voids of the porous scaffold can be equivalent to the volume of water absorption, and the amount of porosity was calculated as follows:

$$P = \frac{W_w - W_d}{V_s} \quad (1)$$

3 Results and discussion

3.1 Scanning electron microscopy

The microstructure of nanocomposite scaffold containing 10 wt% nano bioglass particles is shown in Fig. 2a–c. The SEM images demonstrated uniform porosities of 250–300 μm pore size that is suitable for osteoblast migration [59, 60]. Murphy et al. examined the effect of mean pore size on cell attachment, proliferation and migration in scaffold for bone tissue engineering. They used different pore sizes in the range of 85,120, 164, 190 and 325 μm, and found that the scaffold with 325 μm pore size is more appropriate for bone tissue engineering [59]. In another study, Oh et al. showed that the 290–310 μm pore size is appropriate for bone formation [60]. Figure 2a–c also show the pore interconnectivity which is essential for cell migration, waste removal and nutrient supply to the scaffold in bone tissue engineering [61]. The samples with bioglass nanoparticles were investigated using SEM under higher magnification in order to observe their structure in

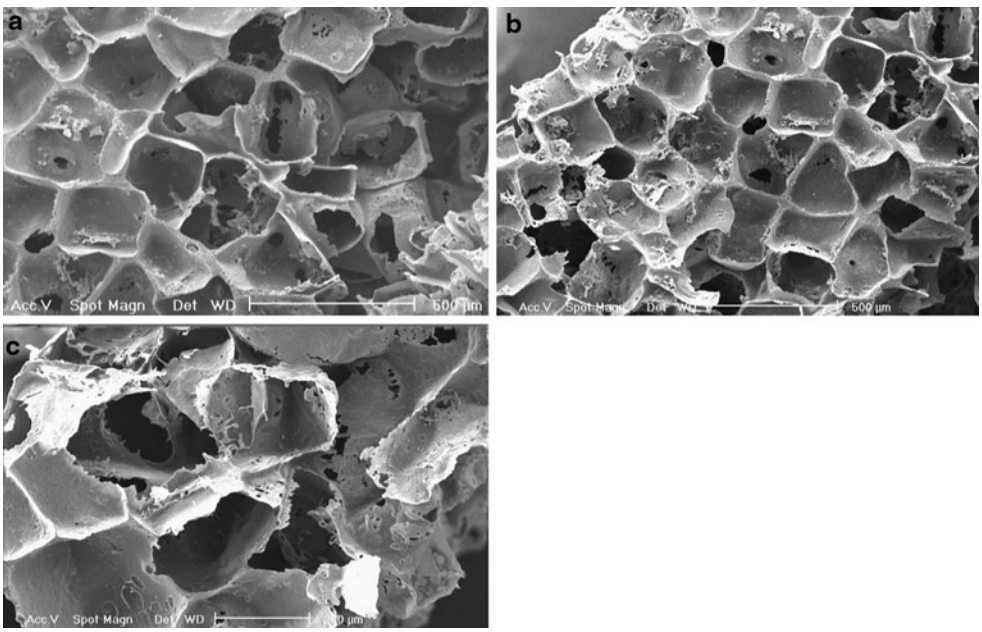

Fig. 2 **a** The SEM of nanocomposite scaffold's surface with 50× magnification. **b** The SEM of nanocomposite scaffold's cross section with 50× magnification. **c** The SEM of nanocomposite scaffold's cross section with 90× magnification

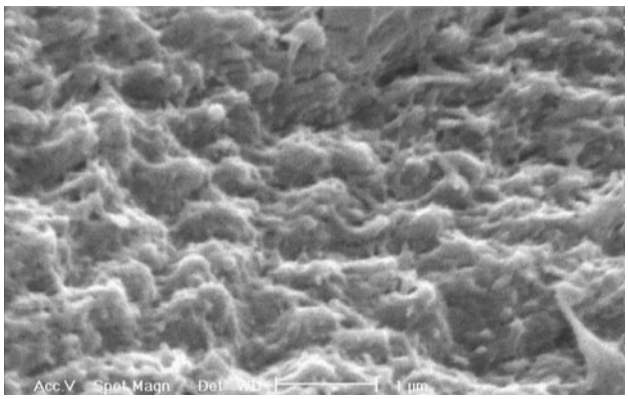

Fig. 3 The SEM of nanocomposite scaffold with 15000× magnification

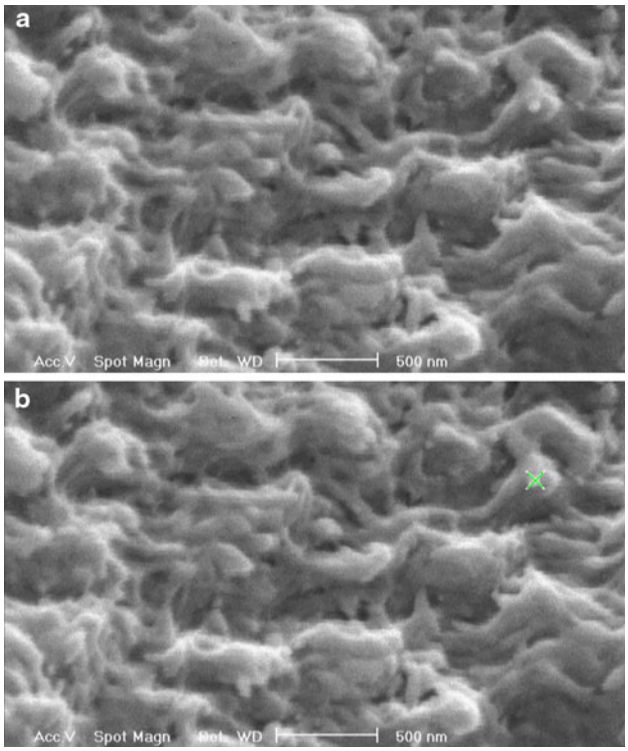

Fig. 4 The SEM of nanocomposite 30000× magnification, the size of nano bioglass is 33 nm

more detail. The results have been shown in Figs. 3 and 4. It can be seen that the particles are constructed by a relatively ordered array of nanoparticles in polymer solution and the prepared nanocomposites exhibit a rough surface that may improve cell attachment (Fig. 3) [62, 63]. The size of nanoparticle that is marked in Fig. 4 is about 33 nm; regarding to the primary particle size of nano bioglass [58], which confirm the lack of agglomeration.

One of the most problematic issues for manufacturing this nanocomposite scaffold is the agglomeration of the bioglass nanoparticles in the PHB matrix because the aggregated bioglass nanoparticles in the composite tend to decrease the mechanical properties and limit its load-bearing applications. Misera et al. proved that composites of PHB with 20 and 30 wt% nano bioglass have less mechanical and biological properties than composites of PHB with 10 wt% nano bioglass [43]. Further pervious studies also showed that using more than 10 wt% nanoparticles of filler in composites cause a recede in mechanical properties [64–66]. Thus, achieving an appropriate method to create PHB/bioglass nanocomposite scaffold has been the key to research work.

Nanomaterials have a high surface-to-volume ratio which is thought to enhance cell adhesion [67, 68]. This is important for cell migration, proliferation, and differentiated function because they are dependant on adhesion [9, 10, 12]. In physiological tissue re-organization (e.g. during wound healing) the bidirectional flow of information exchanged between cells and ECM steers important cell functions such as adhesion, differentiation and migration [69] and should be enhanced in nanomaterials. Based on this, the application of nanomaterials in scaffolds should serve as a better environment for cell attachment, proliferation and function than traditional scaffolds. Therefore, it seems that the nanocomposite scaffold justifies the examination of further tests for bone tissue engineering.

3.2 ATR-FTIR study

The IR transmittance spectra for the $CaO–SiO_2–P_2O_5$ bioglass are shown in Fig. 5. In the figure, four primary vibrational peaks can be seen; the first in the range of 1040–1100 cm^{-1}, the second in the range of 793–814 cm^{-1}, the third in the range of 640–670 cm^{-1} and the fourth in the range of 3410–3430 cm^{-1}.

The higher-frequency vibrations in the range of 1040–1100 cm^{-1} correspond to the modes of the Si–O–Si asymmetric bond stretching vibrations and the lower-frequency modes calculated in the 793–814 cm^{-1} regions to the symmetric Si–O-Si stretching vibrations. The absorption around 950 cm^{-1} is attributed to the Si–O–Ca bonds containing non-bridging oxygen [70]. Ca–O bonds are

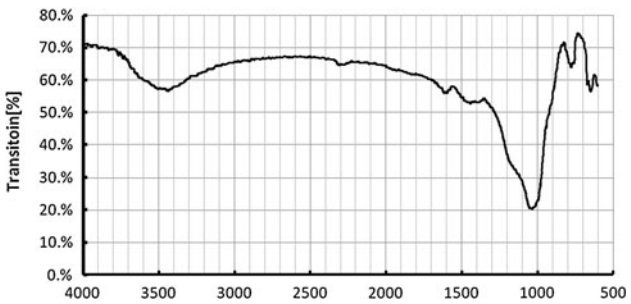

Fig. 5 The FTIR of bioglass

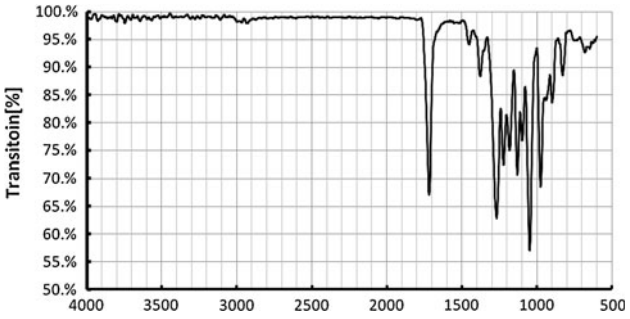

Fig. 6 The FTIR of PHB

observed in 640–670 cm^{-1} region [71]. High-frequency peaks at 3433 cm^{-1} are assigned to O–H stretching of molecular adsorbed water and the peaks around 2362 cm^{-1} are attributed to absorption by the atmospheric CO_2.

The IR transmittance spectra for the poly (3hydroxybutyrate) are shown in Fig. 6. The C=O carbonyl stretching bond of the ester group appears at 1722 cm^{-1}. The bond at about 1380 cm^{-1} is assigned to symmetric wagging of CH_3 groups. The bond at 1230 cm^{-1} is proposed as the conformational bond of the helical chains since no amorphous bonds of the same group could be found. The bonds at 1186 and 1133 cm^{-1} are characteristic of the asymmetric and the symmetric stretching vibration of the C–O–C group, respectively. Other peaks between 800 and 1000 cm^{-1} are assigned the isotactic C–C bond [72].

The IR transmittance spectra for the PHB/bioglass nanocomposite have been shown in Fig. 7. The bond groups of two phases of nanocomposite are presented. In the figure, the Peak of carbonyl groups at 1720 cm^{-1} is smaller than pure PHB; in addition, the peak of Ca–O bonds at about 650 cm^{-1} is more intense than pure bioglass. It seems that there are some interactions between nano bioglass and poly (3hydroxybutyrate); the bonds at about 760 cm^{-1} may be assigned to CaO with the carbonyl group. Moreover, some peaks are shifted which gives more reason to believe that the carbonyls group participates in the interaction with CaO. Therefore, it seems that there is a

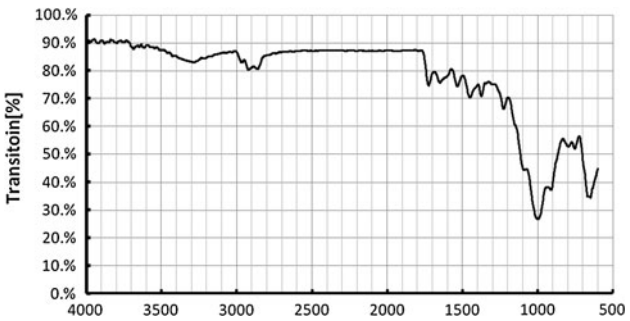

Fig. 7 The FTIR of PHB/bioglass nanocomposite

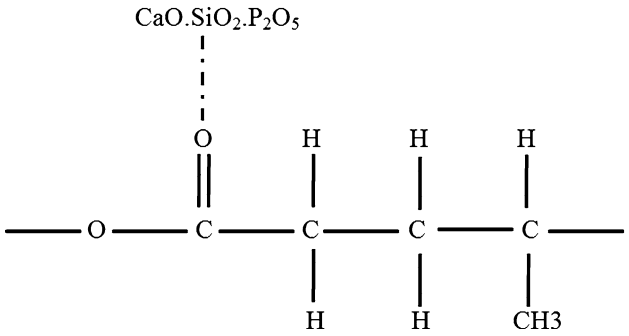

Fig. 8 The bond in the interface of nanocomposite's phases

good bond between nano bioglass and poly (3hydroxybutyrate) in the interface of nanocomposite's phases (Fig. 8).

3.3 DTA study

The DTA results of the four samples are shown in Fig. 9. The curve of nano bioglass powder shows no exothermic and endothermic reactions up to 500°C. In the three other curves, the first endothermic peaks at about 170–180°C represent the melting point of polymer; and the exothermic peaks appear around 270–290°C which is attributed to the combustion and oxidation of polymer. In contrast the melting points of polymer in the PHB curve and the PHB plus bioglass powder (without composition) curve appear to have an equal temperature. When comparing the PHB curve and PHB/bioglass nanocomposite curve, the melting point and combustion process of nanocomposite appear at higher temperature. Leading to the conclusion that there are some connective bonds between polymer and bioglass nanoparticles. The results of DTA analyses confirmed the

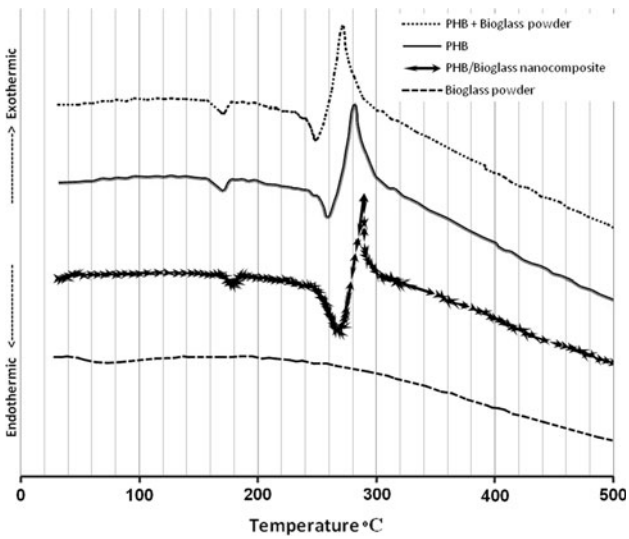

Fig. 9 The DTA of bioglass powder, PHB/bioglass nanocomposite, PHB and PHB + bioglass powder

Table 2 The porosity of scaffold

Sample	*P* (%)
Part1	84.8
Part2	84.7
Part3	84.2

FTIR results and showed a proper interaction in the nanocomposites' phases. Thus, this scaffold can exhibit better mechanical and biological properties based upon the appropriate interaction between phases and the background bioactivity and biocompatibility of each material in nanocomposite.

3.4 Porosity of scaffold

The porosity of scaffold was assessed from three different parts of the sample separately. Part 1 was selected from the middle of the scaffold and the two other parts were selected from different parts of the scaffold and the results are listed in Table 2.

The results demonstrated that the scaffold has uniform porosity in its different parts and the quantity of scaffold porosity is favorable to bone tissue engineering (about 84%). To get a high overall permeability, high-porosity scaffolds are recommended. With increasing porosity, however, the apparent scaffold's stiffness decreases. Sufficient porosity is also essential to reach high permeability for waste removal and nutrient supply to the scaffold from the surrounding healthy bone [73].

4 Conclusion

In this study, the novel nanocomposite scaffold was prepared with 10 wt% bioglass, and the SEM images demonstrated that the scaffold possesses less agglomeration and has rough surfaces that may improve cell attachment. In addition, the FTIR and DTA results showed that it seems that there is a favorable interaction between polymer and bioglass nanoparticles which improves connection in the interface of nanocomposite's phases. Finally, this scaffold has acceptable porosity and morphologic character that warrants further studies to be conducted on the perspective of bone tissue engineering.

References

1. Langer R, Vacanti JP. Tissue engineering. Science. 1993; 260:920–6.
2. Bauer TW, Muschler GF. Bone graft materials. An overview of the basic science. Clin Orthop Relat Res. 2000;371:10–27.
3. Mastrogiacomo M, Muraglia A, Komlev V, Peyrin F, Rustichelli F, Crovace A, et al. Tissue engineering of bone: search for a better scaffold. Orthod Craniofac Res. 2005;8:277–84.
4. Bonfiglio M, Jeter WS. Immunological responses to bone. Clin Orthop Relat Res. 1972;87:19–27.
5. Vacanti JP, Vacanti CA. In: Lanza RP, Langer R, Vacanti J, editors. Principles of tissue engineering. 2nd ed. California: Academic Press; 2000. p. 3.
6. Temenoff JS, Lu L, Mikos AG. In: Davies JE, editor. Bone engineering. Toronto: EM Squared; 2000. p. 455.
7. Laurencin CT, Attawia M, Borden MD. Advancements in tissue engineered bone substitutes. Curr Opin Orthop. 1999;10:445–51.
8. Coombes AG, Meikle MC. Resorbable synthetic polymers as replacements for bone graft. Clin Mater. 1994;17:35–67.
9. Salgada AJ, Coutinho OP, Reis RL. Bone tissue engineering: state of the art and future trends. Macromol Biosci. 2004;4:743–65.
10. Hutmacher DW. Scaffolds in tissue engineering bone and cartilage. Biomaterials. 2000;21(24):2529–43.
11. Guoping C, Takashi U, Tetsuya T. Scaffold design for tissue engineering. Macromol Biosci. 2002;2(2):67–77.
12. Ma PX. Scaffolds for tissue fabrication. Mater Today. 2004; 7(5):30–40.
13. Williams SF, Martin DP, Horowitz DM, Peoples OP. PHA applications: addressing the price performance issue I. Tissue engineering. Int J Biol Macromol. 1999;25:111–21.
14. Zhao K, Deng Y, Chen JC, Chen GQ. Polyhydroxyalkanoate (PHA) scaffolds with good mechanical properties and biocompatibility. Biomaterials. 2003;2:1041–5.
15. Valappil SP, Misra SK, Boccaccini AR, Roy I. Biomedical applications of polyhydroxyalkanoates, an overview of animal testing and in vivo responses. Expert Rev Med Device. 2006;3: 853–68.
16. Chen GQ, Wu Q. The application of polyhydroxyalkanoate as tissue engineering materials. Biomaterials. 2005;26:6565–78.
17. Freier T, Sternberg K, Behrend D, Schmitz KP. Health issues of biopolymers: polyhydroxybutyrate. In: Doi Y, Steinbüchel A, editors. Biopolymers. Weinheim: Wiley-VCH; 2002. p. 247.
18. Reusch RN. Low molecular weight complexed poly(3-hydroxybutyrate): a dynamic and versatile molecule in vivo. Can J Microbiol. 1995;41(Suppl. 1):50–4.
19. Martin DP, Peoples OP, Williams SF, Zhong LH. Nutritional and therapeutic uses of 3-hydroxyalkanoate oligomers. US Patent Appl 359086, 1999.
20. Nebe B, Forster C, Pommerenke H, Fulda G, Behrend D, Bernewski U, et al. Structural alterations of adhesion mediating components in cells cultured on poly b hydroxyl butyric acid. Biomaterials. 2001;22:2425–34.
21. Shishatskaya EI, Volova TG. A comparative investigation of biodegradable polyhydroxyalkanoate films as matrices for in vitro cell cultures. J Mater Sci Mater Med. 2004;15:915–23.
22. Zinn M, Witholt B, Egli T. Occurrence, synthesis and medical application of bacterial polyhydroxyalkanoate. Adv Drug Deliv Rev. 2001;53:5–21.
23. Young RC, Wiberg M, Terenghi G. Poly-3-hydroxybutyrate (PHB): a resorbable conduit for long gap repair in peripheral nerves. Br J Plast Surg. 2002;55:235–40.
24. Novikova LN, Pettersson J, Brohlin M, Wiberg M, Novikov LN. Biodegradable poly-b-hydroxybutyrate scaffold seeded with Schwann cells to promote spinal cord repair. Biomaterials. 2009; 29:1198–206.
25. Fukada E, Ando Y. Piezoelectric properties of poly-b-hydroxybutyrate and copolymers of b-hydroxybutyrate and b-hydroxyvalerate. Int J Biol Macromol. 1986;8:361–6.
26. Knowles JC, Mahmud FA, Hastings GW. Piezoelectric characteristics of polyhydroxybutyrate based composite. Clin Mater. 1991;8:155–8.

27. Zhao Y, Zou B, Shi Z, Wu Q, Che GQ. The effect of 3-hydroxybutyrate on the in vitro differentiation of murine osteoblast MC3T3-E1 and in vivo bone formation in ovariectomized rats. Biomaterials. 2007;28:3063–73.
28. Galego N, Rozsa C, Sanchez R, Fung J, Vazquez A, Tomas JS. Characterization and application of poly(b-hydroxyalkanoates) family as composite biomaterials. Polym Test. 2000;19:485–92.
29. Misra SK, Valappil SP, Roy I, Boccaccini AR. Polyhydroxyalkanoate (PHA)/inorganic phase composites for tissue engineering applications. Biomacromolecules. 2006;7:2249–58.
30. Ni J, Wang M. In vitro evaluation of hydroxyapatite reinforced polyhydroxybutyrate composite. Mater Sci Eng C-Bio S. 2002; 20:101–9.
31. Luklinska ZB, Bonfield W. Morphology and ultrastructure of the interface between hydroxyapatite-polyhydroxybutyrate composite implant and bone. J Mater Sci Mater Med. 1997;8:379–83.
32. Misra SK, Nazhat SN, Valappil SP, Torbati MM, Wood RJK, Roy I, et al. Fabrication and characterization of biodegradable poly(3-hydroxybutyrate) composite containing Bioglass. Biomacromolecules. 2007;8:2112–9.
33. Fisher JP, Mikos AG, Bronzino GD. Tissue engineering: nanocomposite scaffolds for tissue engineering. CRC Press; 2007. p 11.
34. Wei G, Ma PX. Structural and properties of nano-hydroxyapatite/polymer composite scaffolds for bone tissue engineering. Biomaterials. 2004;25:4749–57.
35. Wanga H, Lia Y, Zuoa Y, Lib J, Mab S, Chenga L. Biocompatibility and osteogenesis of biomimetic nano-hydroxyapatite/polyamide composite scaffolds for bone tissue engineering. Biomaterials. 2007;28:3338–48.
36. Guan D, Chen Z, Huang C, Lin Y. Attachment, proliferation and differentiation of BMSCs on gas-jet/electrospun nHAP/PHB fibrous scaffolds. Appl Surf Sci. 2008;255:324–7.
37. Ginebra MP, Driessens FCM, Planell JA. Effect of the particle size on the micro and nanostructural features of calcium phosphate cement: a kinetic analysis. Biomaterials. 2004;25:3453–62.
38. Kalita SJ, Bhardwaj A, Bhatt HA. Nanocrystalline calcium phosphate ceramics in biomedical engineering. Mater Sci Eng C. 2007;27:441–9.
39. Zhang F, Lin K, Chang J, Lu J, Ning C. Spark plasma sintering o macro-porous calcium phosphate scaffolds from nano-crystalline powders. J Eu Ceram Soc. 2008;28(3):539–45.
40. Vollenweider M, Brunner TJ, Knecht S, Grass RN, Zehnder M, Imfeld T, et al. Remineralization of human dentin using ultrafine bioactive glass particles. Acta Biomater. 2007;3:936–43.
41. Brunner TJ, Grass RN, Stark WJ. Glass and bioglass nanopowders by flame synthesis. Chem Commun. 2006;13:1384–6.
42. Rhee SH, Choi JY. Preparation of a bioactive poly (methyl methacrylate)/silica nanocomposite. J Am Ceram Soc. 2002;85: 1318–20.
43. Misra SK, Mohn D, Brunner TJ, Stark WJ, Philip SE, Roy I, et al. Comparison of nanoscale and microscale bioactive glass on the properties of P(3HB)/Bioglass composites. Biomaterials. 2008; 29:1750–61.
44. Hong Z, Reis RL, Mano JF. Preparation and in vitro characterization of scaffolds of poly(L-lactic acid) containing bioactive glass ceramic nanoparticles. Acta Biomater. 2008;4:1297–306.
45. Lu X, Lv X, Sun Z, Zheng Y. Nanocomposites of poly(L-lactide) and surface-grafted TiO_2 nanoparticles: synthesis and characterization. Eur Polym J. 2008;44:2476–81.
46. Torres FG, Nazhat SN, Md Sheikh, Fadzullah SH, Maquet V, Boccaccini AR. Mechanical properties and bioactivity of porous PLGA/TiO_2 nanoparticle-filled composites for tissue engineering scaffolds. Compos Sci Technol. 2007;67:1139–47.
47. Boccaccini AR, Gerhardt LC, Rebeling S, Blaker JJ. Fabrication, characterization and assessment of bioactivity of poly (D, L-lactid acid) (PDLLA)/TiO_2 nanocomposite films. Compos Part A-Appl S. 2005;36:721–7.
48. Cooper CA, Ravich D, Lips D, Mayer J, Wagner HD. Distribution and alignment of carbon nanotubes and nanofibrils in a polymer matrix. Comp Sci Technol. 2002;62:1105–12.
49. Misra1 SK, Watts PCP, Valappil1 SP, Silva SRP, Roy I, Boccaccini AR. Poly(3-hydroxybutyrate)/Bioglass_composite films containing carbon nanotubes. Nanotechnology. 2007;18:075701(7 pp).
50. Grausova L, Kromka A, Bacakova L, Potocky S, Vanecek M, Lisa V. Bone and vascular endothelial cells in cultures on nanocrystalline diamond films. Diam Relat Mater. 2008;17:1405–9.
51. Palin E, Liu HN, Webster TJ. Mimicking the nanofeatures of bone increases bone-forming cell adhesion and proliferation. Nanotechnology. 2005;16:1828–35.
52. Wilson J, Pigot GH, Schoen FJ, Hench LL. Toxicology and Biocompatibility of bioglass. J Biomed Mater Res. 1981;15:805–11.
53. Oonishi H, Kutrshitani S, Yasukawa E, Iwaki H, Hench LL, Wilson J, et al. Particulate bioglass compared with hydroxyapatite as a bone graft substitute. Clin Orthop Relat Res. 1997; 334:316–25.
54. Maquet V, Boccaccini AR, Pravata L, Notingher I, Jerome R. Porous poly(a-hydroxyacid)/bioglasss composite scaffolds for bone tissue engineering. I: preparation and in vitro characterisation. Biomaterials. 2004;25:4185–94.
55. Boccaccini AR. Bioresorbable and bioactive composite materials based on polylactide foams filled with and coated by Bioglasss particles for tissue engineering applications. J Mater Sci Mater Med. 2003;14:350–443.
56. Gatti AM, Valdre G, Andersson OH. Analysis of the in vivo reactions of a bioactive glass in soft and hard tissue. Biomaterials. 1994;15:208–12.
57. Fathi MH, Doostmohammadi A. Preparation and characterization of sol–gel bioactive glass coating for improvement of biocompatibility of human body implant. Mat Sci Eng A-Struct. 2008; 474:128–33.
58. Fathi MH, Doostmohammadi A. Bioactive glass nanopowder and bioglass coating for biocompatibility improvement of metallic implant. J Mater Process Tech. 2009;209:1385–91.
59. Murphy CM, Haugh MG, O'Brien FJ. The effect of mean pore size on cell attachment, proliferation and migration in collagen-glycosaminoglycan scaffolds for bone tissue engineering. Biomaterials. 2010;31:461–6.
60. Oh SH, Park K, Kim JM, Lee JH. In vitro and in vivo characteristics of PCL scaffolds with pore size gradient fabricated by a centrifugation method. Biomaterials. 2007;28(9):1664–71.
61. Petite H, Quarto R. Engineered bone: tissue engineering of bone. Eurekah.com; 2005. p. 108.
62. Deligianni DD, Katsala N, Ladas S, Sotiropoulou D, Amedee J, Missirlis YF. Effect of surface roughness of the titanium alloy Ti-6Al-4V on human bone marrow cell response and on protein adsorption. Biomaterials. 2001;22:1241–51.
63. Kunzler TP, Drobek T, Schuler M, Spencer ND. Systematic study of osteoblast and fibroblast response to roughness by means of surface-morphology gradients. Biomaterials. 2007;28: 2175–82.
64. Boissard CIR, Bourban PE, Tami AE, Alini M, Eglin D. Nanohydroxyapatite/poly(ester urethane) scaffold for bone tissue engineering. Acta Biomater. 2009;5:3316–27.
65. Deng C, Wen J, Lu X, Zhou SB, Wan JX, Qu SX, et al. Mechanism of ultrahigh elongation rate of poly(D, L-lactide)-matrix composite biomaterial containing nano-apatite fillers. Mater Lett. 2008;62:607–10.
66. Zhu ZK, Yang Y, Yin J, Qi ZN. Preparation and properties of organosoluble polyimide/silica hybrid materials by sol–gel process. J Appl Polym Sci. 1999;73:2977–84.

67. Matthews JA, Wnek GE, Simpson DG, Bowlin GL. Electrospinning of collagen nanofibers. Biomacromolecules. 2002;3(2):232–8.
68. Boland ED, Matthews JA, Pawlowski KJ, Simpson DG, Wnek GE, Bowlin GL. Electrospinning collagen and elastin: preliminary vascular tissue engineering. Front Biosci. 2004;9:1422–32.
69. Lutolf MP, Hubbell JA. Synthetic biomaterials as instructive extracellular microenvironments for morphogenesis in tissue engineering. Nat Biotechnol. 2005;23(1):47–55.
70. Pappas GS, Liatsi P, Kartsonakis IA, Danilidis I, Kordas G. Synthesis and characterization of new SiO_2–CaO hollow nanospheres by sol–gel method: bioactivity of the new system. J Non-Cryst Solids. 2008;354:755–60.
71. Shajan XS, Mahadevan C. FT-IR spectroscopic and thermal studies on pure and impurityadded calcium tartrate tetrahydrate crystals. Cryst Res Technol. 2005;40:598–602.
72. Xua J, Guoa BH, Yanga R, Wub Q, Chenb GQ, Zhang ZM. In situ FTIR study on melting and crystallization of polyhydroxyalkanoates. Polymer. 2002;43:6893–9.
73. Sanz-Herrera A, Garcia-Aznar JM, Doblare M. A mathematical model for bone tissue regeneration inside a specific type of scaffold. Biomech Model Mech. 2008;7:355–66.